RESEARCH ARTICLE

Molecular Reproduction & Development 80:297–314 (2013)

Transcriptomic Signature to Oxidative Stress Exposure at the Time of Embryonic Genome Activation in Bovine Blastocysts

GAEL L.M. CAGNONE AND MARC-ANDRÉ SIRARD*

Département des Sciences Animales, Centre de Recherche en Biologie de la Reproduction, Université Laval, Québec, Canada

ABSTRACT

In order to understand how in vitro culture affects embryonic quality, we analyzed survival and global gene expression in bovine blastocysts after exposure to increased oxidative stress conditions. Two pro-oxidant agents, one that acts extracellularly by promoting reactive oxygen species (ROS) production (0.01 mM 2,2′-azobis (2-amidinopropane) dihydrochloride [AAPH]) or another that acts intracellularly by inhibiting glutathione synthesis (0.4 mM buthionine sulfoximine [BSO]) were added separately to in vitro culture media from Day 3 (8–16-cell stage) onward. Transcriptomic analysis was then performed on resulting Day-7 blastocysts. In the literature, these two pro-oxidant conditions were shown to induce delayed degeneration in a proportion of Day-8 blastocysts. In our experiment, no morphological difference was visible, but AAPH tended to decrease the blastocyst rate while BSO significantly reduced it, indicating a differential impact on the surviving population. At the transcriptomic level, blastocysts that survived either pro-oxidant exposure showed oxidative stress and an inflammatory response (*ARRB2*), although AAPH induced higher disturbances in cellular homeostasis (*SERPINE1*). Functional genomics of the BSO profile, however, identified differential expression of genes related to glycine metabolism and energy metabolism (*TPI1*). These differential features might be indicative of pre-degenerative blastocysts (*IGFBP7*) in the AAPH population whereas BSO exposure would select the most viable individuals (*TKDP1*). Together, these results illustrate how oxidative disruption of pre-attachment development is associated with systematic up-regulation of several metabolic markers. Moreover, it indicates that a better capacity to survive anti-oxidant depletion may allow for the survival of blastocysts with a quieter metabolism after compaction.

* Corresponding author:
Pavillon des services
INAF, bureau 2732
Université Laval
Québec, Canada G1V 0A6.
E-mail: marc-andre.sirard@fsaa.ulaval.ca

Grant sponsor: NSERC; Grant sponsor: Strategic Network Embryo GENE; Grant number: NETPG 340825-06

Mol. Reprod. Dev. 80: 297–314, 2013.

Received 15 November 2012; Accepted 7 February 2013

Published online 5 April 2013 in Wiley Online Library (wileyonlinelibrary.com).
DOI 10.1002/mrd.22162

Additional supporting information may be found in the online version of this article.

Abbreviations: AAPH, 2,2′-azobis (2-amidinopropane) dihydrochloride; BSO, buthionine sulfoximine; DEG, differentially expressed gene; GSH, reduced glutathione; ICM, inner cell mass; IVC, in vitro culture; IVP, in vitro-produced; MET, maternal-to-embryonic transition; VIVO, in vivo-produced. **Genes**: *ACTA1/2*, actin, alpha 1 (skeletal muscle)/2 (smooth muscle, aorta); *ACTB*, actin, beta; *ACTC1/2*, actin, alpha, cardiac muscle 1/2; *ACTG2*, actin, gamma 2, smooth muscle, enteric; *ARRB2*, arrestin, beta 2; *ERK1/2*, mitogen-activated protein kinase 3/1; *GCSH*, glycine cleavage system protein H (aminomethyl carrier); *GJA1*, gap junction protein, alpha 1, 43 kDa; *HEY2*, hairy/enhancer-of-split related with YRPW motif 2; *HIF1A*, hypoxia inducible factor 1, alpha subunit; *IFNA2*, interferon, alpha 2; *IFNT*, interferon, tau; *IGF2*, insulin-like growth factor 2 (somatomedin A); *IGFBP7*, insulin-like growth factor binding protein 7; *IL5*, interleukin 5; *JAM2*, junctional adhesion molecule 2; *KRAS*, v-Ki-ras2 Kirsten rat sarcoma viral oncogene homolog; *LUM*, lumican; *MKL1*, megakaryoblastic leukemia (translocation) 1; *MMD*, monocyte to macrophage differentiation-associated; *MYL6/7*, myosin, light chain 6 (alkali, smooth muscle and non-muscle)/7 (regulatory); *NFKB*, nuclear factor of kappa light polypeptide gene enhancer in B-cells; *NRF2*, nuclear factor (erythroid-derived 2)-like 2; *OLR1*, oxidized low density lipoprotein (lectin-like) receptor 1; *PDGFC*, platelet derived growth factor C; *PLOD2*, procollagen-lysine, 2-oxoglutarate 5-dioxygenase 2; *PPIA*, peptidylprolyl isomerase A (cyclophilin A); *PTPLAD1*, protein tyrosine phosphatase-like A domain containing 1; *RHOC*, ras homolog family member C; *RNF20*, ring finger protein 20, E3 ubiquitin protein ligase; *SERPINE1*, serpin peptidase inhibitor, clade E (nexin, plasminogen activator inhibitor type 1), member 1; *SF3B1*, splicing factor 3b, subunit 1, 155 kDa; *TGF[B3]*, transforming growth factor [beta 3]; *THBS1*, thrombospondin 1; *TKDP1*, Trophoblast Kunitz domain protein 1; *TNF*, tumor necrosis factor; *TNFSF9*, tumor necrosis factor (ligand) superfamily, member 9; *TPI1*, triosephosphate isomerase 1; *YWHAB*, tyrosine 3-monooxygenase/tryptophan 5-monooxygenase activation protein, beta polypeptide; *ZFAND5*, zinc finger, AN1-type domain 5

INTRODUCTION

In assisted reproductive technology (ART), the suboptimal environment encountered by early embryos during in vitro culture (IVC) is one cause of poor blastocyst quality. Moreover, IVC is associated with long-term effects on health, as demonstrated by the higher incidence of developmental syndromes in the ART-offspring population (Alukal and Lipshultz, 2008), notably in bovine pregnancies which are sometimes associated with high birth-weight calves (large offspring syndrome) and peri-natal mortality (Young et al., 1998; Farin et al., 2006). Although numerous changes have been made to IVC protocols, the complex interactions between medium composition, physical equilibrium, and incubation conditions are still sub-optimal for proper embryo development. As a result, early developmental deviation during IVC could correlate with the developmental origins of health and disease hypothesis (Lazzari et al., 2002). Therefore, investigation is required to measure the impact of IVC on embryonic plasticity in regards to the reduced blastocyst quality.

In the last decade, the advancement of functional genomics and the capacity to work with minute samples have allowed the study of gene expression in the early embryo. During the first cleavages, transcription is largely silent, and early metabolism is supported by the transcripts and proteins provided by the oocyte. This phase of transcriptomic quiescence is followed by activation of the embryonic genome, which corresponds to the maternal-to-embryonic transition (MET; 8–16-cell stage in bovine). Transcription of the embryonic genome following the MET is extremely dynamic, controling morula compaction and subsequent blastocyst development (Hamatani et al., 2006; Rodriguez-Zas et al., 2008). Numerous studies have shown the range of gene expression modulation under different IVC conditions (Duranthon et al., 2008; Smith et al., 2009). While transcriptional changes may be required for the embryo to adapt its homeostasis to the environmental conditions, it is believed that perturbations of developmentally important genes may translate into a stress response affecting embryonic quality (Rizos et al., 2002) although the genes related to the embryonic stress response need further characterization.

We hypothesized that analyzing the transcriptomic profile of embryos cultured under enhanced stress conditions would define specific gene patterns associated with compromised quality. Moreover, defining markers of embryonic stress response may allow the development of alternative strategies towards an empirical reformulation of culture conditions.

The maintenance of oxidative homeostasis, that is, the equilibrium between reactive oxygen species (ROS) production and anti-oxidant defence, is critical for normal cell division and differentiation. In vivo, the oviduct provides the optimal red/ox environment for the embryo to maintain its oxidative homeostasis. This is supported by the limited free radical content in the environment, the normal stimulation of oxidative metabolism, and the availability of anti-oxidant molecules (Guerin et al., 2001). IVC affects oxidative homeostasis (Gardiner et al., 1998; Agarwal et al., 2006) by increasing ROS exposure or mitigating anti-oxidant protection, thereby resulting in lower embryo quality. For instance, variations in oxygen concentration (Lequarre et al., 2003; Rodina et al., 2009) and temperature (Sakatani et al., 2008) have been shown to modulate the rate of ROS production while supplementation with antioxidant molecules could counteract oxidative stress during IVC (Takahashi et al., 1993; Liu et al., 1999). Accordingly, ROS have deleterious effects on cell constituents, organelles, and developmental kinetics that may, in turn, affect implantation success (Agarwal et al., 2006).

Considering the important impact of oxidative stress on IVC, previous reports analyzed the effect of exposure to pro-oxidant agents (2,2′-azobis (2-amidinopropane) dihydrochloride [AAPH] or buthionine sulfoximine [BSO]) during post-compaction development of bovine embryos (Takahashi et al., 1993; Feugang et al., 2003, 2005). With a half-life of 175 hr in a hydrophilic environment, AAPH is known to induce continuous free radical formation that initiates cell membrane lipid peroxidation and generates ROS. BSO, on the other hand, inhibits the key enzyme of glutathione synthesis, gamma-glutamylcysteine synthase, and results in depletion of cellular glutathione (GSH) content in bovine oocytes and embryos (Takahashi et al., 1993; de Matos et al., 1996). BSO activity could be maintained for 5 days in culture medium. Here, exposure to AAPH or BSO was tested during post-compaction development (from Day 3 to Day 7), a period when embryonic homeostasis is challenged by increasing oxidative metabolism (Fischer and Bavister, 1993; Donnay and Leese, 1999; Thompson, 2000) and low glutathione content (Gardiner and Reed, 1994, 1995b). The objective of this study was to gain insight as to how the embryonic genome responds to mild extracellular or intracellular oxidative stress. This is the first report using this type of analysis.

RESULTS

Differential Impact of AAPH and BSO Exposure on Blastocyst Survival

In order to investigate the impact of oxidative stress on early bovine development, in vitro-produced (IVP) bovine zygotes were cultured in control conditions until Day 3. Afterwards, zygotes were transferred to either control or treatment conditions containing a pro-oxidant agent, either AAPH or BSO, and cultured until Day 7. Phenotypically visible results were not present at the morula stage (Day 5). The blastocyst rate was not significantly affected by 0.01 mM AAPH treatment, but was significantly reduced after exposure to 0.4 mM BSO ($P = 0.04$; Fig. 1). Higher standard deviation in the blastocyst rate was noted in AAPH replicates (9.8%) compared to BSO (6.4%) or control replicates (4.4%). The hatching rate of Day-7 blastocysts was not significantly affected by either pro-oxidant agent when compared to control. Moreover, no visible impact on embryo morphology was observed in blastocysts produced in each treatment.

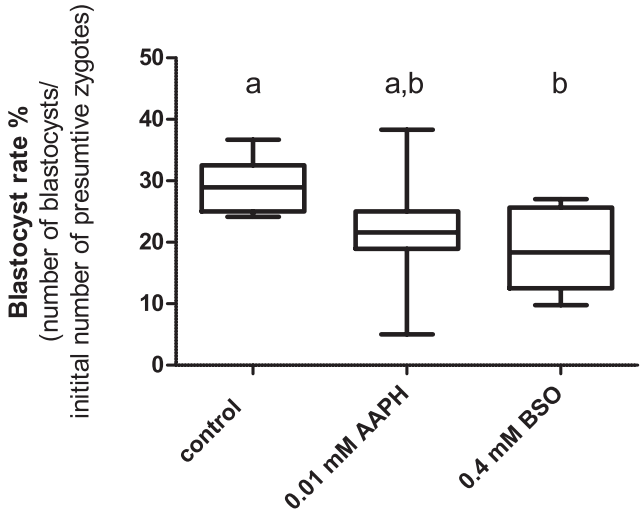

Figure 1. Survival rate in pro-oxidant conditions. Data represent the mean blastocyst rate (±standard deviation) after IVC exposure to control, 0.01 mM AAPH, or 0.4 mM BSO-supplemented conditions during post-compaction development (Days 3–7). Different superscripts represent a significant difference between groups (ANOVA $P < 0.05$).

Gene Expression Profile in Blastocysts after AAPH or BSO Exposure

Microarray technology was used for large-scale assessment of bovine embryo gene expression in response to mild oxidative stress. Of the 38,732 gene-targeted probes that cover the microarray slides, more than 17,000 probes exhibited an intensity signal higher than the summation of background intensity plus two standard deviations, regardless of the treatment. Only these probes were considered for genomics analysis.

Statistical analysis of gene expression differences between treatments and controls was performed using a Limma test, which determined a *P*-value and fold-change for all the genes expressed in AAPH and BSO blastocysts compared to control (CTL). Flexarray tools generated a scatter plot of *P*-values that depicts the number of differentially expressed genes (DEGs; probe count) against intervals of *P*-value (interval of 0.0125), irrespective of the fold-change. Results showed a higher number of DEGs in low-*P*-value ranges (<0.05) for BSO compared to AAPH (Fig. 2A). A scatter plot of fold-change was also generated with the fold-change of all the DEGs from AAPH and BSO, irrespective of *P*-value. In this plot, the identity line would correspond to 100% correlation in DEG fold-changes in both treatments. Results demonstrated a correlation of DEG fold-change of $R^2 = 0.36$ and a preferential abundance of DEGs under the identity line, that is, in the AAPH treatment (Fig. 2B).

Significant differential expression was considered for probes showing a symmetrical fold-change superior to ± 1.5, with significance at $P < 0.05$. With these criteria, 226 and 476 probes were shown to be differentially expressed in AAPH- and BSO-treated blastocysts, respectively (Fig. 2C). In AAPH-treated blastocysts, 70.7% (160/226) of DEGs were up-regulated, while 60.2% (287/476) of DEGs were down-regulated in BSO-treated blastocysts. Sixty-four DEGs overlapped both AAPH and BSO conditions. When symmetrical fold-change cut-off was set at ± 2 ($P < 0.05$), AAPH-treated blastocysts had 59 DEGs (55 up- and 4 down-regulated) while BSO-treated blastocysts had 40 DEGs (8 up- and 32 down-regulated genes). With these criteria, only 5 DEGs were common to AAPH and BSO treatments. AAPH-related DEGs showed a higher interval of fold-change (from -2.24 to 7.15) compared to BSO-related ones (-3.2 to 5.19). Lumican was the most up-regulated gene in both treatments.

To validate the microarray results, a total of 11 genes, including four housekeeping genes (*ACTB*, *MYL6*, *PPIA*, *YWHAB*) plus seven predicted DEGs (*ARRB2*, *GCSH*, *IFNT*, *SERPINE1*, *TKDP1*, *TPI1*, *IGFPB7*) were analyzed by reverse transcriptase-quantitative PCR on three independent samples (Fig. 3). Housekeeping genes (HKG) were selected according to their levels of expression, their fold-changes/*P*-values from the Limma comparison between control and treated blastocysts (fold-change $< \pm 1.1$, $P > 0.5$), and their functions (not directly implicated in the signaling pathways of the oxidative stress response). GeNorm results calculated consistent expression of *ACTB*, *MYL6*, and *PPIA* throughout conditions. AAPH-predicted DEGs were *ARRB2*, *SERPINE1*, and *IGFBP7*, while BSO-predicted DEGs were *ARRB2*, *TKDP1*, *TPI1*, *GCSH*, and *IFNT*. The use of an ANOVA statistical test validated the difference ($P = 0.05$) in relative expression for two out of three selected DEGs from the AAPH treatment (*ARRB2*, *IGFBP7*) and three out of five selected DEGs from the BSO treatment (*ARRB2*, *TKDP1*, *TPI1*). The AAPH treatment had a non-significant impact in gene expression of *SERPINE1* ($P = 0.44$), although the AAPH-related variance was significantly different compared to control or BSO groups.

Overlapping DEGs Associated With Different Physiological Status/Developmental Conditions

As the impact of oxidative stress has been potentially associated with the skewing of sex ratio in early embryos (Feugang et al., 2005), the proportion of AAPH- and BSO-related DEGs that could be associated with embryonic sex were determined (Bermejo-Alvarez et al., 2010). Among annotated AAPH- and BSO-related DEGs, only 7.0% (8/113) and 7.3% (17/230), respectively, moderately overlapped with sex-related genes; the association of more sex-specific targeted genes with the treatments may have indicated a sex-effect in addition to the treatment effect.

Increased oxidative stress has been associated with mitochondrial stress in hyperglycemia-treated embryos (Hashimoto et al., 2000; Leunda-Casi et al., 2002; Karja et al., 2006). Therefore, we determined the proportion of AAPH- and BSO-related DEGs that overlapped with the list of 63 DEGs previously described in high-glucose treated blastocysts (Cagnone et al., 2012). Among AAPH-related

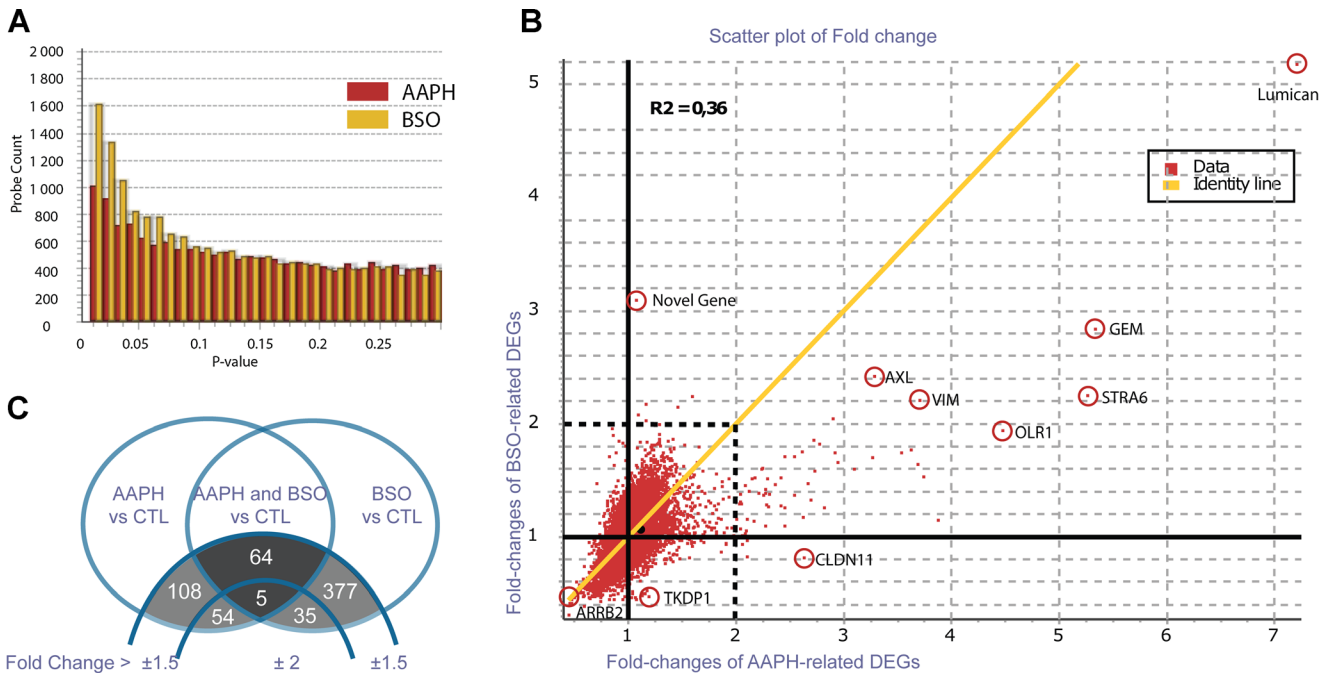

Figure 2. Microarray analysis of differential gene expression profiles in blastocysts from AAPH and BSO conditions compared to control. **A**: Data represent the number of differentially expressed genes (probe) in AAPH or BSO groups when compared to control, as a function of the corresponding *P*-value. **B**: Data represent the scatter plot of all DEG fold-changes induced by AAPH and BSO. **C**: Venn diagram representing the number of DEGs in AAPH- and/or BSO-treated blastocysts with $P < 0.05$ and fold-change $>\pm 1.5$ compared to control (CTL).

DEGs, 34 showed a consistent overlap with energetic stress-related genes (Fig. 4A) and resulted in a significant correlation of fold-change ($R = 0.83$, $P < 0.0001$, results not shown). Among BSO-related DEGs, only three showed consistent overlap with energetic stress-related genes with similar fold-changes.

Since increased oxidative stress has been associated with lower embryo quality, the proportion of AAPH- and BSO-related DEGs that correspond to the DEGs from comparison of in vivo-(VIVO) and in vitro-produced (IVP) bovine blastocysts was determined. This correspondence was possible since the reference IVP blastocysts for both pro-oxidant and VIVO transcriptomic comparisons were derived using an identical in vitro production protocol from a consistent batch of abbatoir ovary's oocytes. Among the genes detected with significant intensity, VIVO blastocysts showed 3,002 DEGs (fold-change $> \pm 1.5$, $P < 0.05$) when compared to IVP blastocysts, with 1,587 down-regulated DEGs and 1,415 up-regulated DEGs. When subjected to overlapping analysis, the AAPH-related profile had 96 DEGs in common with the VIVO profile (Fig. 4B), most of which were up-regulated in AAPH and down-regulated in VIVO when compared to control (Fig. 4C). In contrast, BSO treatment showed 160 DEGs in common with VIVO (Fig. 4B) most of which were both up- or down-regulated when compared to control (Fig. 4D). Only seven DEGs showed a common association with both pro-oxidants and VIVO. These DEGs showed inconsistent fold-changes, except for the up-regulated gene lumican, which was highly down-regulated in VIVO (-13.4, $P = 0.015$).

Pathway Analysis of AAPH and BSO Gene Expression Profiles

DAVID analysis software significantly clustered DEGs into functionally related groups. AAPH-related DEGs clustered with extracellular matrix organization and cell adhesion, and BSO-related DEGs clustered with structural constituents of ribosomes and glycolysis. Ingenuity Pathway Analysis revealed a significant enrichment of AAPH-related DEGs throughout 14 canonical pathways. The first five pathways were: coagulation system, TGF-beta signaling, hepatic fibrosis, pattern recognition of bacteria/viruses, and atherosclerosis signaling. BSO-related DEGs were significantly associated with 38 canonical pathways, and the top five pathways were: EIF2 (eukaryotic translation initiation factor 2) signaling, inositol metabolism, NRF2-mediated oxidative stress response, clathrin-mediated endocytosis signaling, and regulation of actin-based motility by rho. The 64 DEGs overlapping AAPH and BSO treatment were not significantly associated with any canonical pathways. DEGs that were specific to each pro-oxidant treatment did not reveal any association with new canonical pathways, although up-regulated genes in BSO-treated blastocysts showed a significant association with function in glycine catabolism and estrogen receptor signaling.

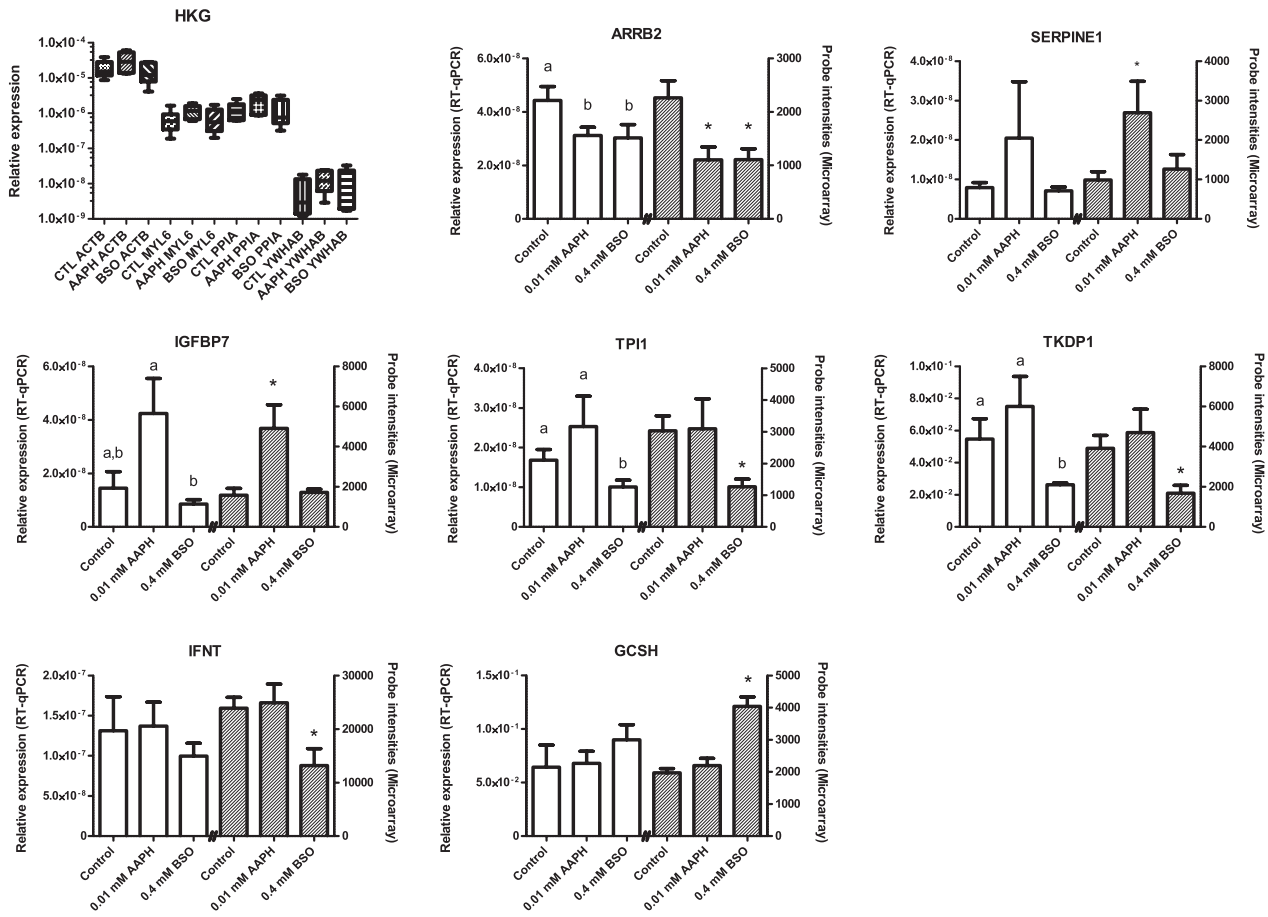

Figure 3. Reverse transcriptase-quantitative PCR results on selected candidates from microarray analysis. Graphs represent the gene expression analysis performed in independent samples using RT-qPCR (white bars) as well as the corresponding probe intensities from microarray results (gray bars). Different superscripts represent significant difference between groups (ANOVA $P < 0.05$). $^{*}P < 0.05$, ANOVA was done on normalized data (see Materials and Methods Section). HKG, housekeeping genes: ACTB, actin beta; MYL6, myosin, light chain 6, alkali, smooth muscle and non-muscle; PPIA, peptidylprolyl isomerase A (cyclophilin A); YWHAB, tyrosine 3-monooxygenase/tryptophan 5-monooxygenase activation protein, beta polypeptide. ARRB2, arrestin beta 2; GCSH, glycine cleavage system protein H (aminomethyl carrier); IFNT, interferon, tau; IGFBP7, insulin-like growth factor binding protein 7; SERPINE1, serpin peptidase inhibitor, clade E (nexin, plasminogen activator inhibitor type 1), member 1; TKDP1, Trophoblast Kunitz domain protein 1; TPI1, triosephosphate isomerase 1.

From the list of DEGs associated with AAPH treatment, the first gene network generated by Ingenuity Pathway Analysis represented the impact of ROS on inflammatory response, and was annotated with cancer and infectious and respiratory disease (Fig. 5, network 1). The second AAPH-related DEG network represented the impact of ROS on energetic metabolism, and was annotated with organism injury and abnormalities, cardiovascular disease, and cancer (Fig. 5, network 2). Twelve genes in this network overlapped with DEGs associated with high glucose stress in bovine blastocysts (*GJA1*, *HIF1A*, *IGF2*, *JAM2*, *LUM*, *MMD*, *OLR1*, *PDGFC*, *PLAT*, *PLOD2*, *SERPINE1*, and *THBS1*). Networks 1 and 2 were both associated with ROS induction of NFKB signaling. The first five potential upstream regulators of total AAPH-related DEGs were endogenous signaling of retinoic acid (activated), KRAS enzyme activity (inhibited), IFNA2 signaling (activated), lipopolysaccharide effect (activated), and TNF (tumor necrosis factor) signaling (activated).

The first networks established from the list of DEGs associated with BSO treatment were annotated to cell cycle, cellular compromise and death, and protein synthesis (Fig. 6). The second network was associated with developmental functions of cellular assembly and organization, and tissue development. Interestingly, this network overlapped with 10 DEGs associated with in vivo-(VIVO) compared to in vitro-produced (IVP) blastocysts (*TNFSF9*, *RNF20*, *SF3B1*, *ZFAND5*, *RHOC*, *ACTA2*, *ACTA1*, *ACTC1*, *ACTC2*, and *MYL7*), as well as NRF2-mediated oxidative stress response (*ACTA1*, *ACTA2*, *ACTC1*, *ACTG2*, and *PTPLAD1*). The first potential up-stream regulators of total BSO-related DEGs were rapamycin (activated), synthetic

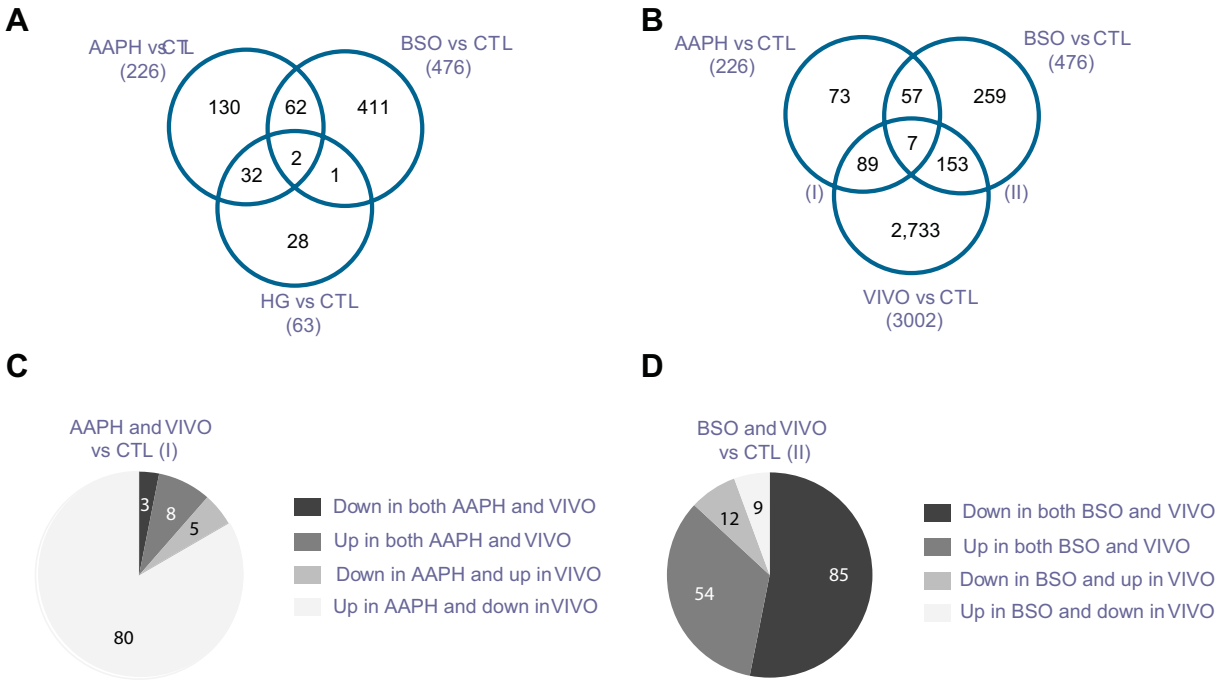

Figure 4. Overlapping DEGs in bovine blastocysts resulting from different conditions of culture. Using control IVP embryos as the same reference for each microarray analysis, Venn diagrams represent the DEGs in AAPH- and BSO-treated blastocysts that overlap the DEGs in high glucose (HG)-treated blastocysts (**A**) or in vivo (VIVO)-produced blastocysts (**B**). Based on common DEGs only, pie charts represent the proportion of DEGs related to AAPH (**C**) or BSO (**D**) treatment that exhibit similar or different expression fold-changes to DEGs related to VIVO treatment.

retinoid CD437, MKL1 (inhibited), and IL5 and HEY2 (activated).

DISCUSSION

The data presented in this work illustrate the genomic response of mammalian embryos to mild oxidative stress, and reveal how they become compromised, especially those that survive the stress. This is the first study exploring this concept with global gene analysis in cattle.

Pro-oxidant agents AAPH and BSO were selected to establish mild stress conditions because they were shown to affect blastocysts in a dose-dependent manner (Feugang et al., 2003, 2005). AAPH generates two potent ROS, alkoxyl (RO−) and peroxyl (ROO−) radicals, that are similar to those physiologically active during IVC and that initiate extra- and intracellular responses to oxidative stress (Guerin et al., 2001). Our first result showed that adding 0.01 mM AAPH during post-compaction did not affect the Day-7 blastocyst rate or subsequent hatching rate. After the MET, several cellular mechanisms regulate the adaptability to ROS and allow the early embryo to resist an increasing dose of oxidative stress caused by AAPH exposure (Stover et al., 2000). The effect of AAPH is, however, apparent at Day 8 when a proportion of produced blastocysts start to degenerate (Feugang et al., 2003), suggesting a delayed impact on oxidative metabolism and differences in the individual capacity to overcome oxidative stress. In our study, we did not observe morphological differences in the Day-7 blastocyst population, consistent with the result of Feugang et al. (2003) showing the appearance of a degenerative phenotype at Day 7.5. AAPH treatment induced considerable variability on the blastocyst rate, however, which could be indicative of differences in weekly IVC runs. Embryo survival rate is sensitive to inherent stress during IVC, and culture conditions are rapidly modulated by oxygen exposure (Agarwal et al., 2006; Martin-Romero et al., 2008). These independent variables could have exacerbated the fluctuating impact of ROS on embryo survival after AAPH treatment.

BSO, an inhibitor of glutathione synthase, was chosen to stress the limited anti-oxidant protection coming from the oocyte that might serve to adapt to IVC conditions. Our results show that post-compaction exposure to 0.4 mM BSO significantly decreased the Day-7 blastocyst rate, which is consistent with another study showing impairment of blastocyst development after 24-hr exposure to 1 mM BSO at the 6–8-cell stage (Takahashi et al., 1993). During post-compaction development, oxidative metabolism is increased to sustain energy production, but embryonic anti-oxidant defence would normally scale accordingly and maintain homeostasis. Glutathione metabolism during early development, however, would have a limited effect in the presence of BSO (Gardiner and Reed, 1995b). Thus, individuals with higher oxidative metabolism or lower

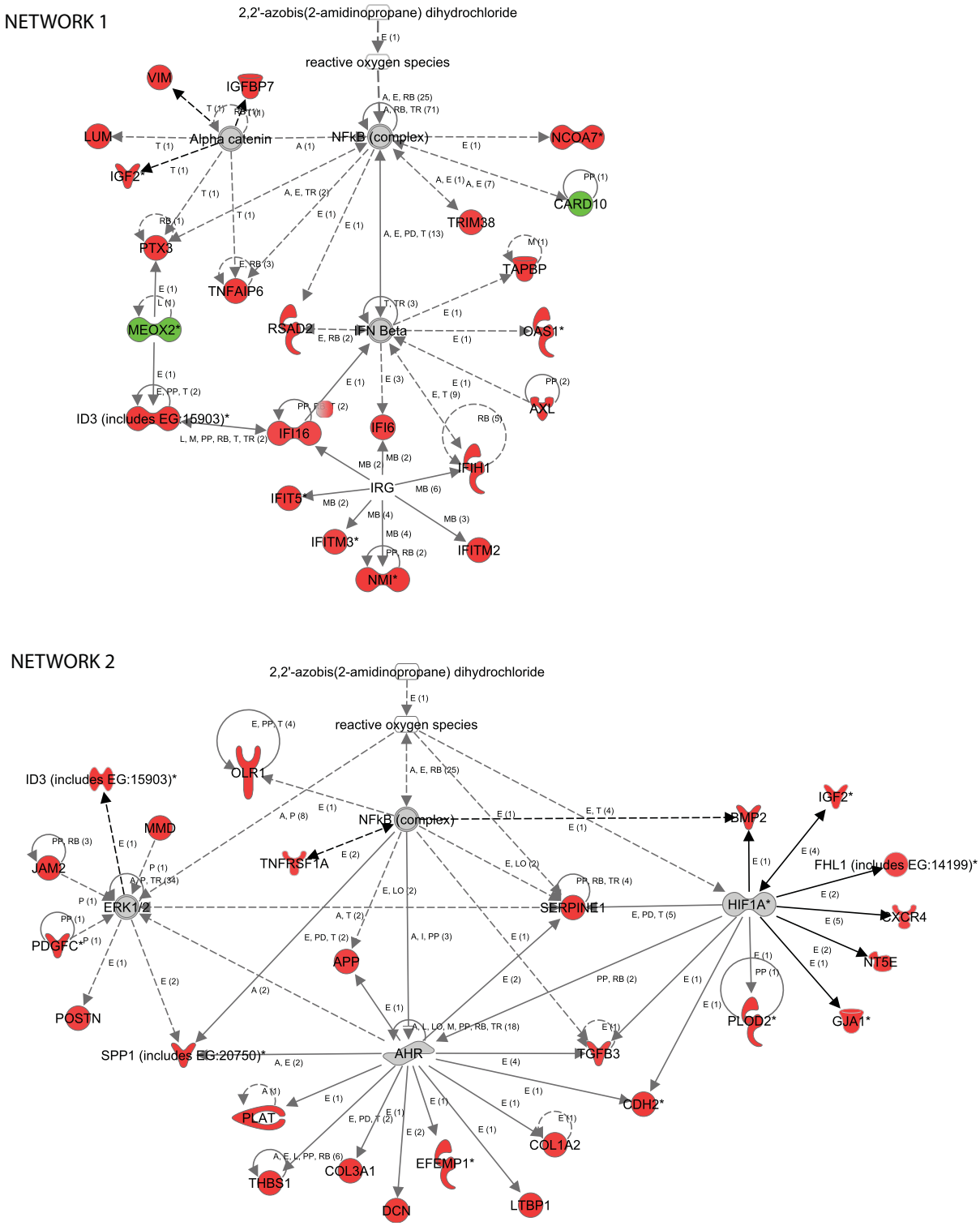

Figure 5. Ingenuity Pathway Analysis of AAPH impact. Based on gene expression connectivity, networks 1 and 2 show the significant associations of DEGs from AAPH-treated blastocysts with the inflammatory response to oxidative stress (network 1) and the impact on mitochondrial metabolism and extracellular matrix fibrosis (network 2). Red and green colors respectively represent up- and down-regulated DEGs in AAPH-treated blastocysts.

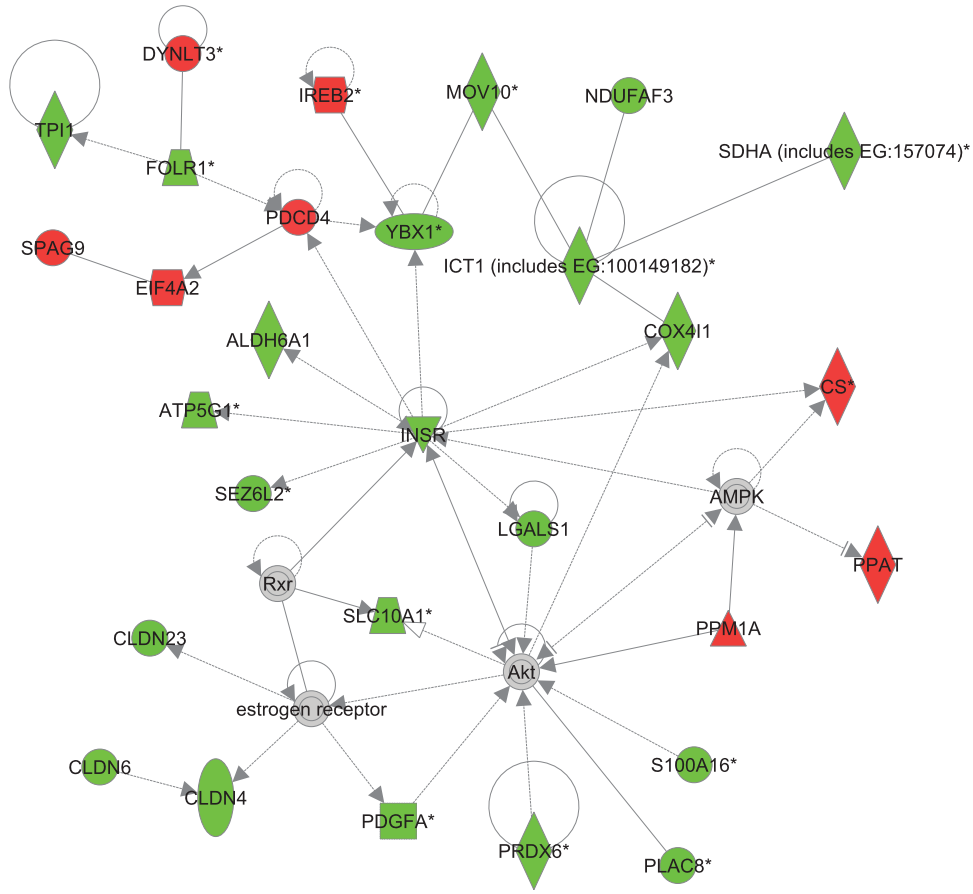

Figure 6. Ingenuity Pathway Analysis of BSO impact. Network representing the associations between BSO-related DEGs, based on the literature knowledge provided by Ingenuity Pathway Analysis. Links between molecules are based on gene expression connectivity as well as experimental proofs of co-functionality. Red and green colors respectively represent up- and down-regulated DEGs in BSO-treated blastocysts.

anti-oxidant competence may suffer from oxidative damage after GSH depletion, and could exhibit developmental arrest at the morula stage (Gardiner and Reed, 1995a). Interestingly, Feugang et al. (2005) showed that, similar to AAPH, 0.4 mM BSO induced dose-dependent blastocyst degeneration apparent at Day 8. In our study, the earlier impact may be due to the absence of serum in the medium and to the potential embryotrophic effect of growth factors that can compensate for homeostatic unbalance (Kurzawa et al., 2004; Lott et al., 2011). Moreover, BSO would have a more stringent effect than AAPH on the red/ox equilibrium maintenance of less-competent blastocysts, which would normally degenerate on Day 8.

To study the mechanisms underlying the impact of oxidative stress on embryo survival, separate transcriptomic analyses were used to compare AAPH- and BSO-treated blastocysts against controls. Results showed a high amplitude in the transcriptomic response of AAPH-treated blastocysts, but also exhibited more variability. In contrast, BSO-treated blastocysts showed moderate modifications in gene expression and higher consistency. This indicates more highly disturbed physiology in AAPH-surviving blastocysts compared to the BSO population. Also, it highlights differences in profile uniformity among AAPH- or BSO-treated blastocysts. Emerging evidence suggests that transcriptomic profiles are widely susceptible to intrinsic variability among the same pool of embryos with close resemblance (Smith et al., 2007). The different survival rates after both pro-oxidant treatments may be associated with a broader range of responses among individuals from the AAPH-treated population, and a reduction in individual transcriptomic diversity after BSO selection. Consistent with our microarray results, AAPH replicates showed a greater standard deviation than BSO replicates in gene expression, as assessed by reverse-transcriptase quantitative PCR on selected candidates such as SERPINE1.

Transcriptomic analysis requires cautious interpretation as the correspondence between mRNA and protein level has not been demonstrated. Nevertheless, identification of particular pathways significantly enriched with differentially expressed genes would indicate the global response to pro-oxidant treatment. Here, AAPH and BSO showed moderate overlapping impact on gene expression in surviving blastocysts. Among common DEGs, lower expression was

validated for *ARRB2*, a gene coding for arrestin B2 that is involved in the modulation of G protein coupled receptor (GPCR) internalization. Recruitment of ARRB2 to beta2-adrenergic receptor induces ROS generation through ERK1/2 (mitogen-activated protein kinase 3/1) signaling (Singh and Moniri, 2012). Interestingly, *ARRB2* loss-of-function is associated with higher activation of MAPK (mitogen-activated protein kinase) after chemokine (C-X-C motif) receptor 2 (CXCR2) activation (Zhao et al., 2004). Here, *CXCR4* was up-regulated after AAPH-treatment. CXCR4 is the GPCR of stromal cell-derived factor (SDF-1, or chemokine (C-X-C motif) ligand 12), which is used by trophoblast cells and acts through ERK1/2 to promote survival. Alterations in *SDF-1* and/or *CXCR4* expression may be associated with pregnancy disorders (Jaleel et al., 2004). In relation to SDF-1 signaling, carma3 (*CARD10*) was down-regulated in both AAPH and BSO treatments. Carma3 is part of the molecular complex that plays a critical role in SDF-1/CXCR4-dependent induction of Nf-KB (nuclear factor of kappa light polypeptide gene enhancer in B-cells) and the survival of carcinoma (Rehman and Wang, 2009; Brzoska et al., 2011). The differential expression of *ARRB2, CXCR4*, and *CARD10* would implicate ERK1/2 in promoting survival in response to oxidative stress.

Carma3 functions with ARRB2 to mediate the pro-inflammatory signal of Nf-KB in endothelial cells (Delekta et al., 2010), and oxidative stress is known to trigger inflammation in somatic tissue (Cui et al., 2004). Here, both AAPH- and BSO-related transcriptomes indicate an inflammatory response in surviving blastocysts. Particularly, TNF signaling, which is central in inflammation, was well represented in AAPH-related DEGs. *TNFAIP8L3* (TNF alpha-induced protein 8-like 3) has been shown to be up-regulated in energetically stressed blastocysts (Cagnone et al., 2012), as were the TNF receptor (*TNFRSF1A)*, the adipokine-coding gene *C1QTNF3* (C1q and tumor necrosis factor related protein 3), and the receptor of oxidized lipoprotein 1. These genes are linked with oxidative stress and inflammation of adipose tissue. As AAPH exposure results in increased cell membrane permeabilization in bovine blastocysts (Yoshida et al., 2004; Feugang et al., 2005), up-regulation of inflammation-responsive genes may be correlated with ROS-induced lipid peroxidation and production of oxidized lipids (Kim et al., 2010; Kopp et al., 2010).

Compared to BSO, AAPH showed a greater impact on inflammatory-associated genes. Coding for the prototypic, evolutionarily conserved, long pentraxin 3, *PTX3* is unequivocally involved in innate immunity and inflammation (Deban et al., 2011). *PTX3* is also up-regulated in cumulus cells just prior to ovulation (in mouse, human, and cow) and, as the cumulus cells are rapidly destroyed by the oviduct afterward, could act as a suicide signal. In addition, several interferon-responsive genes were up-regulated after AAPH, such as interferon-induced transmembrane proteins 2 and 3 (*IFITM2* and *3*), whose encoded proteins are involved in cell adhesion during embryogenesis (Siegrist et al., 2011). Interestingly, *IFITM3* expression is restricted to the inner cell mass (ICM) and is up-regulated in cloned bovine blastocysts (Smith et al., 2007). As *IFITM3* over-expression reduces proliferation in human cell lines, it may affect ICM growth in AAPH-treated blastocysts. Moreover, IFITM3 physically interacts with secreted phosphoprotein 1 (SPP1, or osteopontin; El-Tanani et al., 2010), a cytokine and adhesion molecule up-regulated at the RNA level in both AAPH- and BSO-treated blastocysts. In response to oxidative stress in vitro and in vivo (Urtasun et al., 2012), *SPP1* down-regulation is associated with enhanced trophoblastic growth and migration during human implantation (Hannan and Salamonsen, 2008). Therefore, analysis of cytokine secretion could be a useful marker of the pro-inflammatory signal before implantation (Johnson et al., 2003).

AAPH- and BSO-treated blastocysts showed common DEGs associated with extracellular matrix signaling and adhesion molecules. Coding for secreted proteoglycans, lumican was up-regulated in both conditions while decorin expression was only increased after AAPH treatment. ROS stimulate the production of advanced glycosylation end-products (AGE) that up-regulate the expression of lumican and decorin (Brownlee, 2001; Schaefer et al., 2001; Pantaleon et al., 2010). Similarly, AGE induces protein glycosylation of the transcription factor SP1 (Brownlee, 2001) and leads to the up-regulation of collagen 3A1 (Santra et al., 2008; Luna et al., 2009), as observed in AAPH-treated blastocysts. Betaglycan and extracellular matrix molecules play an important role in extracellular signaling and in the regulation of TGF-beta activity (Massague and Chen, 2000). Here, expression of *TGFB3* was increased in AAPH-treated blastocysts. Up-regulation of *TGFB3* may predispose pregnancy to preeclampsia whereas reduced expression is linked to trophoblastic invasiveness (Caniggia et al., 1999). Similarly, *NDP*, encoding the putative extracellular factor Norrin with homology to the TGF-beta super family, was up-regulated after AAPH exposure and would have an important role in reproductive tissues around implantation and possibly in the embryo (Luhmann et al., 2005). Along with TGF-beta and other extracellular matrix factors (Edwards, 2012), analyzing the external signal produced by the embryos could indicate a potential inflammatory response (Lohr et al., 2012) with the subsequent attraction of neutrophils, which may be detrimental for implantation (Hayashi et al., 2010).

As for inflammation, AAPH induced a higher impact than BSO on extracellular matrix remodeling. Periostin, a matrix protein involved in cell adhesion as well as tissue remodeling, was up-regulated after AAPH exposure. Highly expressed during fibrosis, increased periostin expression could result from an inflammatory signal through several cytokines such as TGF-beta (Marotta et al., 2009; Yang et al., 2012). Moreover, AAPH treated blastocysts up-regulated thrombospondin, a gene coding for a glycoprotein in the extracellular matrix found at the porcine maternal-fetal interface (Edwards et al., 2011) that binds several ligands, including glycosaminoglycans as well as plasminogen. Interestingly, genes involved in plasminogen function were up-regulated after AAPH exposure. Plasminogen

activator inhibitor (SERPINE1) and tissue-type plasminogen activator (PLAT) control the proteolytic degradation of plasminogen and modulation of thrombosis. Under oxidative stress conditions, secretion of SERPINE1 and PLAT is associated with ERK1/2 activation (Banfi et al., 2003). Furthermore, TGFB3 induces expression of collagen (Verrecchia and Mauviel, 2002) and *SERPINE1* (Liu, 2008) during fibrosis. Plasminogen activity was suggested to participate in implantation (Kubo et al., 1981; Aflalo et al., 2004), and differential expression of *SERPINE1* during placental oxidative stress is associated with pre-eclampsia (Meade et al., 2007; Wikstrom et al., 2009). Changes in gene expression relative to extracellular matrix proteases may have important consequences at the time of attachment and could be associated with miscarriage after IVC.

With implications to fibrosis-like remodeling, the AAPH-related profile is associated with growth-factor signaling. Up-regulated in AAPH-treated blastocysts, platelet-derived growth factor-C (PDGFC) regulates numerous genes involved in tissue remodeling and organogenesis (Jinnin et al., 2005). *PDGFC* is up-regulated in growing uterine fibroids (Suo et al., 2009) and is inversely correlated with lymphocyte infiltration in carcinomas (Bruland et al., 2009). *PDGFC receptor* is expressed by early embryos, suggesting at least a paracrine effect on the proliferation of the ICM and derived tissues (Osterlund et al., 1996). PDGF supplementation would partially rescue TNF-alpha/IFN-gamma induction of trophoblast apoptosis (Smith et al., 2002). Similarly, insulin-like growth factor 2 (IGF2), up-regulated in AAPH-treated blastocysts, has been shown to rescue embryo development after exposure to oxidative stress (Smith et al., 2002; Kurzawa et al., 2004; Kawamura et al., 2007; Artus et al., 2010). IGF signaling plays a fundamental role in embryonic-maternal crosstalk and in early embryo development (Thieme et al., 2012). *IGF2* is up-regulated in ovine parthenotes (Bebbere et al., 2010) as well as in hyperglycemia-treated blastocysts in rabbit (Thieme et al., 2012) and cattle (Cagnone et al., 2012). Considering that growth factors for the ICM play a key role in activating the ERK pathway, *PDGF* and *IGF2* up regulation may counteract inflammatory signal and maintain survival after oxidative stress.

Both AAPH- and BSO-related profiles indicate the impact of oxidative stress, but surviving blastocysts exhibited different anti-oxidant responses. On the one hand, AAPH-treated blastocysts show up-regulation of anti-oxidant enzymes. Methionine sulfoxide reductase beta 3 (Weissbach et al., 2002) responds to peroxide-induced cellular oxidation of methionine (Chao et al., 1997; Zhang et al., 2011) while glutathione peroxidase 8 (Guerin et al., 2001) eliminates the methionine sulfoxidation caused by AAPH (Cui et al., 2011; Nguyen et al., 2011). On the other hand, BSO-related DEGs indicated a significant representation of nrf2 signaling. The Nrf2 transcription factor is involved in mediating the response to oxidative stress after BSO treatment (Lee et al., 2008). Yet, the BSO-related DEGs, concordant with Nrf2 targets, were mostly down-regulated in blastocysts. For example, the gene coding for the stress-induced phosphoprotein that coordinates the folding activity of chaperones was down-regulated, as were two heat shock protein (HSP) genes. This suggests that while AAPH-treated blastocysts exhibit an anti-oxidant response, embryos that survived BSO treatment would have better anti-oxidant capacity and therefore lower Nrf2 activity (Lee et al., 2008).

Instead of an antioxidant response, BSO-treated blastocysts showed an up-regulation of genes coding for two glycine cleavage system proteins involved in the catabolism of amino acids. Glycine is the enzymatic substrate of the γ-glutamyl-cystein synthase, which produces the reduced glutathione and is specifically inhibited by BSO. It has been demonstrated that preimplantation embryos can up-regulate de novo GSH synthesis in response to oxidative stress, but not to GSH depletion (Stover et al., 2000). Therefore, inhibition of GSH turnover would increase glycine content (Zhang et al., 2009) which, although required to maintain embryonic cell osmolarity in culture (Baltz and Tartia, 2010), may still be damaging for cellular homeostasis (Leipnitz et al., 2009). Thus, the up-regulation of the glycine cleavage system could improve the clearance of glycine accumulation (Oda et al., 2007) as a side effect of inhibited GSH synthesis. Accordingly, serine hydroxymethyltransferase 1 (*SHMT1*) expression was down-regulated in both AAPH- and BSO-treated blastocysts. This serine dehydrogenase catalyzes the reversible conversion of serine and tetrahydrofolate to glycine and 5,10-methylene tetrahydrofolate. Moreover, folate receptor 1, a membrane-bound receptor responsible for uptake of folate in human embryonic stem cells and bovine embryos (Steele et al., 2005; Kwong et al., 2010), was down-regulated in BSO-treated blastocysts. Folate is a methyl donor, and depletion of folate results in elevated intracellular cystein and GSH. Although further studies are required to validate changes in amino acid content in BSO-treated embryos, differential expression of genes related to glycine and folate turnover may have potential implication in methyl group metabolism in surviving blastocysts.

Feugang et al. (2005) showed that blastocysts surviving AAPH or BSO treatments exhibit comparable hatching rates, mean cell numbers, and apoptotic cell rates, while degenerating embryos have higher cellular and molecular damage. Here, AAPH-treated blastocysts had more impact on the inflammatory response than their BSO counterparts. IFN-gamma/TNF-alpha induced apoptosis under PI3K (phosphatidylinositol-4,5-bisphosphate 3-kinase) signaling in trophoblast and early embryos (Kawamura et al., 2007; Loureiro et al., 2007), and up-regulation of responsive genes may be correlated with increased apoptotic rate in degenerating blastocysts (Feugang et al., 2003). In addition, *ID3*, which codes for the inhibitor of differentiation/DNA binding 3, was up-regulated in AAPH-treated blastocysts. ID3 acts under p38/MAPK as a redox sensor of cell proliferation in response to increased ROS (Mueller et al., 2002; Nickenig et al., 2002). In sheep, *ID3* is up-regulated in degenerated blastocysts as part of the transcriptomic regulation of TGF-beta signaling (Li et al., 2012). The different gene expression patterns between AAPH-

and BSO-surviving blastocysts lead us to hypothesize the existence of a differential contribution of pre-degenerating blastocysts in each pro-oxidant comparison.

The notion elaborated in the quiet hypothesis proposes that embryos with internal damage exhibit a more active metabolic state than embryos able to maintain normal homeostasis (Leese et al., 2007). AAPH- and BSO-treated blastocysts showed opposing profiles when compared to high-glucose treated blastocysts (Cagnone et al., 2012). High glucose is thought to induce metabolic stress by targeting mitochondrial function (Chi et al., 2002), and increasing the expression of glycolytic enzymes, a pathologic enhancement of the Warburg effect during post-compaction development (Marin-Hernandez et al., 2009; Cagnone et al., 2012; Krisher and Prather, 2012). The Warburg effect corresponds to the use of aerobic glycolysis as a complementary source of building blocks and energy to mitochondrial respiration. Here, AAPH increased the expression of *IGFBP7*, a gene coding for the secreted IGF-binding protein 7, which reflects metabolic perturbation of mitochondrial oxidative phosphorylation in mammalian somatic and cancer cells (Cervera et al., 2009). These perturbations are concomitant with ROS production, which induces NFκB signaling pathways as well as activation of the AhR/HIF1A (aryl hydrocarbon receptor/, hypoxia inducible factor 1, alpha subunit) complex (De Palma et al., 2007; Harvey et al., 2002), an important site of cross-talk at the level of transcription in AAPH-related gene networks (Dimova et al., 2004; Meade et al., 2007).

In contrast to AAPH, BSO-surviving blastocysts showed up-regulation of the tricarboxylic acid (TCA)-related citrate synthase gene, but down-regulated expression of aldolase A, fructose-bisphosphate (*ALDOA*), which is involved in glucose metabolism and is positively associated with a higher glycolytic rate (Sugiura et al., 2005; Paczkowski and Krisher, 2010). We also observed down-regulation of *TPI1*, which codes for a triose phosphate isomerase, an important glycolytic enzyme under the regulation of HIF1A in conditions of metabolic stress (Hamaguchi et al., 2008). Lower glycolitic activity in the BSO group could also be related to the lower expression of the insulin receptor (*INSR1*), a positive marker of diabetes and obesity (Cai et al., 2012). Taken together, these differential patterns of metabolic genes suggest that AAPH impacts mitochondrial oxidation and therefore energy production. In contrast, lower expression of glycolytic enzymes may translate to efficient oxidative activity in BSO-surviving blastocysts.

Overall gene up-regulation is concomitant with the environmental stress response to IVC conditions when compared to the in vivo environment (Lazzari et al., 2002; Cote et al., 2011; Robert et al., 2011). Associated with major up-regulation of gene expression (>70%), AAPH treatment enhanced the impact of IVP when compared to VIVO production system, and the majority of these genes were associated with inflammatory response. In contrast, the majority (>60%) of BSO-related DEGs were down-regulated and showed similar changes as observed in VIVO blastocysts. Cautious interpretation is required as common DEGs from pro-oxidant-surviving blastocysts represent a low percentage of those found between IVP and VIVO blastocysts. However, this transcriptomic similarity coincides with a major down-regulation of ribosomal genes in the BSO group. Under the control of the nucleolus, and representing a high proportion of total RNA content, ribosomal RNA abundance has been associated with embryo quality (Zheng et al., 2012). Moreover, ribosomal RNA synthesis during blastocyst development would be kept low in quiet and more viable embryos (El-Sayed et al., 2006; Leese et al., 2007).

With regard to viability, two genes inversely related to developmental competence (*TKDP1* and *ANXA2)* were down-regulated in either BSO or VIVO blastocysts when compared to IVP controls. Annexin 2 (*ANXA2*), a calcium-dependent phospholipid binding protein involved in membrane fusion and signal transduction, is correlated to be up-regulated in pregnancy loss and abortion (El-Sayed et al., 2006). Moreover, aberrant expression of *ANXA2* in trophoblastic cells during decidualization leads to pro-inflammatory signaling and preeclampsia (Menkhorst et al., 2012). TKDP1 is hypothesized to function as a maternal-recognition factor, and both *TKDP 3* and *4* are up-regulated in blastocysts derived from IVC as compared to artificial insemination (Smith et al., 2009). Little is known about the function of the TKDP family members, but their temporal expression profile and localisation at the fetal-maternal interface strongly suggests a role during pregnancy (Chakrabarty and Roberts, 2007). Prior to any embryo transfer experiment, the differential expression of competence markers by BSO-treated blastocysts may indicate higher embryonic quality in the surviving population. Testing the metabolic state of blastocysts that survive BSO treatment is required to validate any potential selection of the best embryos after GSH depletion.

In conclusion, our analysis showed that both extra- and intra-cellular oxidative stress disrupted pre-attachment development, and that surviving blastocysts showed transcriptomic modifications associated with inflammation and extracellular matrix remodeling, featuring a fibrosis-like reaction similar to that seen in somatic tissues (Bhattacharyya et al., 2012). Although required for adaptability, this stress response may profoundly alter cellular signaling by either inducing embryo degeneration or affecting subsequent maternal recognition. In addition, genomic analysis of the BSO-related profile suggests a response to high glycine in blastocysts after glutathione depletion. Moreover, these surviving blastocysts showed lower expression of metabolic genes like their in vivo counterparts (quiet hypothesis), suggesting a selection of better quality embryos based on their capacity to maintain homeostasis after antioxidant depletion. More investigations are required to ensure that stress response does not affect the potentially higher viability of BSO-selected individuals.

MATERIALS AND METHODS

All chemicals were obtained from Sigma–Aldrich (Oakville, Ontario, Canada), unless otherwise stated.

In Vitro Production of Bovine Blastocysts

Oocyte collection and in vitro maturation Cumulus–oocyte complexes (COCs) were obtained by aspirating follicles from the ovaries of slaughtered heifers. After four washes in TLH (HEPES-buffered Tyrode's Lactate solution), groups of up to 10 selected COCs with at least five layers of cumulus were placed in 50-μl drops of medium under mineral oil in dishes (Nunc, Roskilde, Denmark), and matured for 24 hr at 39°C under an atmosphere of 5% CO_2 in air with maximum humidity. The maturation medium was TCM-199 supplemented with 10% fetal calf serum (HyClone, ThermoScientific, USA), 0.1 μg/ml of FSH (Folltropin V, Bioniche, Canada), 0.33 mM of pyruvic acid, and 50 μg/ml of gentamycin.

In vitro fertilization Following maturation, five matured COCs were added to 48-μl droplets of in vitro fertilization (IVF) medium under mineral oil. The IVF medium was composed of TL STOCK (Tyrode's Lactate solution) supplemented with 0.6% fatty acid free bovine serum albumin (BSA), 0.2 mM pyruvic acid, 10 μg/ml heparin, and 50 μg/ml gentamycin. Prior to transfer, the COCs were washed twice in TLH medium. Once transferred, 2 μl of PHE (1 mM hypotaurine, 2 mM penicillamine, 250 mM epinephrine) were added to each droplet 10 min before spermatozoa was added. The spermatozoa used consisted of a cryopreserved mixture of ejaculates from five bulls (Centre d'Insémination Artificielle du Québec, St.-Hyacinthe, QC, Canada). The spermatozoa were thawed in 37°C water for 1 min, put on a discontinuous Percoll gradient (2 ml of 45% Percoll over 2 ml of 90% Percoll), and centrifuged at 700*g* for 30 min at 26°C. After discarding the supernatant, the pellet of live spermatozoa was counted on a haemocytometer to obtain a concentration of 10^6 cells/ml, and was resuspended in IVF medium. Finally, 2 μl of the sperm suspension (final concentration $= 4 \times 10^4$ cells/ml) were added to each IVF droplet containing the matured COCs, and was incubated for 16–18 hr in a humidified atmosphere at 38.5°C in 5% CO_2.

In vitro culture For IVC of embryos, a three-step modified synthetic oviduct fluid (SOF) culture system containing MEM, essential and non-essential amino acids, 0.5 mM of glycyl-glutamine, and 0.4% fatty acid-free BSA under embryo-tested mineral oil (#8410, Sigma) was used. The embryo culture dishes were incubated at 38.5°C with 6.5% CO_2, 5% O_2, and 88.5% N_2 in 100% humidity. Briefly, after fertilization, presumptive zygotes were mechanically denuded and washed three times in TLH supplemented with fatty acid-free BSA, then were placed in groups of 10 in 10-μl droplets of SOF1 with non-essential amino acids (1X) and 3 μM EDTA. Embryos were transferred to new 10-μl droplets of SOF2 containing non-essential (1×) and essential (0.5×) amino acids 72 hr post-fertilization, and transferred again 120 hr post-fertilization to 20-μl droplets of SOF3 containing non-essential (1×) and essential (1×) amino acids. The medium was replaced three times to prevent toxicity due to ammonium accumulation and nutrient depletion caused by amino acid degradation and embryo metabolism, respectively. The glucose concentration used in SOF1, 2, and 3 was respectively 0.2, 0.5, and 1.0 mM. Cleavage rate, (number of embryos with at least two cells out of total embryos) and 8/16-cell embryo rate (number of embryos with at least eight cells out of total embryos) were determined during embryo transfer from SOF1 to SOF2 (Day 3). Blastocyst rate (number of early, expanded and hatched blastocysts out of total embryos) and hatching rate (number of hatched blastocysts out of total blastocysts) were calculated at the end of the culture period.

Exposure to pro-oxidant treatments Concentrations of 0.01 mM for AAPH and 0.4 mM for BSO were selected as they appeared to be detrimental for blastocyst development (Feugang et al., 2003, 2005), and were used from Day 3 to produce seven replicates of control, AAPH-, or BSO-treated blastocysts from different in vitro production runs. Blastocyst development was assessed at Day 7 post-fertilization. Pooled blastocysts (hatched and non-hatched) were washed three times in phosphate-buffered saline (PBS), collected in groups of 10 in small volumes of PBS into 0.5 ml microfuge tubes, and stored at −80°C until RNA extraction. Each replicate contained about 10 embryos, including non-expanded (early), expanded, and hatched blastocysts. Equivalent proportions of hatched blastocysts were kept between control and treatment replicates. Four out of seven replicates were used for the microarray experiments and three out of seven replicates were used to validate the microarray results by reverse transcriptase-quantitative PCR (RT-qPCR).

Determination of differential gene expression profile Total RNA from each replicate was extracted and purified using a *PicoPure* RNA Isolation Kit (Life Science, New York, NY). After DNase digestion (Qiagen, Toronto, Ontario, Canada), the quality and concentration of extracted RNA was analyzed with a Bioanalyzer (Agilent, Mississauga, Ontario, Canada). All extracted samples were of good quality, with an RNA Integrity Number >7.5.

For microarray purposes, purified RNA was amplified by in vitro transcription with T7 RNA amplification using the RiboAmp® HS^{Plus} RNA Amplification Kit (Life Science) and labeled with Cy3 and Cy5 using the ULS Fluorescent Labeling Kit (Kreatech, NC). aRNA (825 ng per replicate) was hybridized on the Agilent-manufactured EmbryoGENE slides in a 2-color dye swap design. After 17 hr of hybridization at 65°C, microarray slides were washed for 1 min in Expression Wash Buffer 1 (room temperature), 3 min in gene Expression Wash Buffer 2 (42°C), 10 sec in 100% acetonitrile (room temperature), and 30 sec in Stabilization and Drying Solution (Agilent). Slides were scanned with PowerScanner (Tecan, Mannedorf, Switzerland) and feature extraction was done with Array-pro6.3 (MediaCybernetics, MD). Intensity files were analyzed with FlexArray (Michal Blazejczyk, Mathieu Miron, Robert Nadon (2007).

FlexArray: A statistical data analysis software for gene expression microarrays. Genome Quebec, Montreal, Canada; http://genomequebec.mcgill.ca/FlexArray).

Raw fluorescence intensity data were corrected by background subtraction, then normalized within (green/red) and between each array (Loess and quantile, respectively). Statistical comparison between treatments (AAPH vs. Control or BSO vs. Control) was done with the Limma algorithm, which attributed to each probe a probability to fold-change difference between treatment and control. The data discussed in this publication have been deposited in NCBI's Gene Expression Omnibus and are accessible through GEO Series accession number GSE42281: http://www.ncbi.nlm.nih.gov/geo/query/acc.cgi?acc=GSE42281.

Validation of microarray results was done by RT-qPCR. Total extracted RNA from independent samples (three replicates for each condition) were reverse-transcribed using oligo-dT primer and a qScript Flex cDNA Synthesis Kit (Quanta Biosciences, MD). Specific primers for each selected gene were designed using PrimerQuest^{SM} (Integrated DNA Technologies, Inc., IA), and qPCR was performed using the LightCycler 480® SYBR Green I Master and the LightCycler® 480 System (Roche, Mannhein, Germany). A standard curve composed of five points of the PCR product for each primer pair diluted from 1 pg to 0.1 fg was used for real-time quantification of PCR output. A GeNORM normalization factor (Vandesompele et al., 2002) from expression values of 3 reference genes (ACTB, MYL6, PPIA) was used for data normalization. Moreover, technical variations were assessed and corrected through quantification of an exogenous *GFP* spike introduced at the time of RNA extraction (Vigneault et al., 2004). ANOVA was used for statistical comparison of developmental rate and RT-qPCR results between control, AAPH, and BSO treatments. Primer sequences, product size, annealing temperature and accession numbers are provided in Supplemental Table 1.

Functional analysis of differentially expressed genes Based on Gene Ontology databases reporting transcriptomic analysis in mammalian embryos, Microsoft Access was used to compare the DEGs that are associated with blastocyst sex status (Bermejo-Alvarez et al., 2010) or detected in Day-7 IVP bovine blastocysts exposed to high glucose stress conditions (Cagnone et al., 2012). Moreover, a microarray profile generated with VIVO blastocysts was also compared to AAPH and BSO profiles. VIVO blastocysts resulted from artificial insemination of super-ovulated eggs and embryo flushing on Day 7 after artificial insemination (Plourde et al., 2012). Gene expression in VIVO blastocysts was compared to control blastocysts (CTL), which were produced using the IVP protocol described earlier. Microarray analysis between VIVO and CTL was performed using the experimental procedure described earlier.

DAVID software was used to analyze the functions of differentially expressed genes into clusters (Huang da et al., 2009a,b). Moreover, data were analyzed with Ingenuity Pathways Analysis (IPA) (Ingenuity® Systems, www.ingenuity.com). IPA was used to compile canonical pathways as well as gene product interactions (networks) that were differentially expressed between treatments. We used IPA to build schematic representations of important pathways that were dysregulated in treated blastocysts.

Network generation A dataset containing gene identifiers and corresponding expression values was uploaded into the application. Each identifier was mapped to its corresponding object in Ingenuity's Knowledge Base. A fold-change cut-off of 1.5 with a P-value < 0.05 was set to identify molecules whose expression was significantly differentially regulated. These molecules, called Network Eligible Molecules, were overlaid onto a global molecular network developed from information contained in Ingenuity's Knowledge Base. Networks of Network Eligible Molecules were then algorithmically generated based on their connectivity. Molecules are represented as nodes, and the biological relationship between two nodes is represented as an edge (line). All edges are supported by at least 1 reference from the literature, from a textbook, or from canonical information stored in the Ingenuity Pathways Knowledge Base. Human, mouse, and rat orthologs of a gene are stored as separate objects in the Ingenuity Pathways Knowledge Base, but are represented as a single node in the network. Nodes are displayed using various shapes that represent the functional class of the gene product.

Canonical pathway analysis IPA identified the pathways that were most significant to the dataset from the IPA library of canonical pathways. The significance of the association between the dataset and the canonical pathway was measured in two ways: (1) A ratio of the number of molecules from the dataset that map to the pathway divided by the total number of molecules that map to the canonical pathway is displayed and (2) Fisher's exact test was used to calculate a P-value to determine the probability that the association between the genes in the dataset and the canonical pathway would occur by chance alone. Green and red symbols represent genes respectively down- and up-regulated in treated embryos compared to controls. Gray symbols represent genes with significant expression in blastocysts but no difference between conditions, whereas white symbols represent genes not present on microarray or with below-background intensity.

ACKNOWLEDGMENTS

We would like to thank Isabelle Laflamme and Isabelle Dufort for technical support. The in vivo embryos were provided by L'Alliance Boviteq, Canada. This study was supported by NSERC and The EmbryoGENE network of Canada.

REFERENCES

Aflalo ED, Sod-Moriah UA, Potashnik G, Har-Vardi I. 2004. Differences in the implantation rates of rat embryos developed in vivo and in vitro: Possible role for plasminogen activators. Fertil Steril 81:780–785.

Agarwal A, Said TM, Bedaiwy MA, Banerjee J, Alvarez JG. 2006. Oxidative stress in an assisted reproductive techniques setting. Fertil Steril 86:503–512.

Alukal JP, Lipshultz LI. 2008. Safety of assisted reproduction, assessed by risk of abnormalities in children born after use of in vitro fertilization techniques. Nat Clin Pract Urol 5:140–150.

Artus J, Panthier JJ, Hadjantonakis AK. 2010. A role for PDGF signaling in expansion of the extra-embryonic endoderm lineage of the mouse blastocyst. Development 137:3361–3372.

Baltz JM, Tartia AP. 2010. Cell volume regulation in oocytes and early embryos: Connecting physiology to successful culture media. Hum Reprod Update 16:166–176.

Banfi C, Camera M, Giandomenico G, Toschi V, Arpaia M, Mussoni L, Tremoli E, Colli S. 2003. Vascular thrombogenicity induced by progressive LDL oxidation: Protection by antioxidants. Thromb Haemost 89:544–553.

Bebbere D, Bogliolo L, Ariu F, Fois S, Leoni GG, Succu S, Berlinguer F, Ledda S. 2010. Different temporal gene expression patterns for ovine pre-implantation embryos produced by parthenogenesis or in vitro fertilization. Theriogenology 74: 712–723.

Bermejo-Alvarez P, Rizos D, Rath D, Lonergan P, Gutierrez-Adan A. 2010. Sex determines the expression level of one third of the actively expressed genes in bovine blastocysts. Proc Natl Acad Sci USA 107:3394–3399.

Bhattacharyya S, Wei J, Varga J. 2012. Understanding fibrosis in systemic sclerosis: Shifting paradigms, emerging opportunities. Nat Rev Rheumatol 8:42–54.

Brownlee M. 2001. Biochemistry and molecular cell biology of diabetic complications. Nature 414:813–820.

Bruland O, Fluge O, Akslen LA, Eiken HG, Lillehaug JR, Varhaug JE, Knappskog PM. 2009. Inverse correlation between PDGFC expression and lymphocyte infiltration in human papillary thyroid carcinomas. BMC Cancer 9:425.

Brzoska K, Sochanowicz B, Siomek A, Olinski R, Kruszewski M. 2011. Alterations in the expression of genes related to NF-kappaB signaling in liver and kidney of CuZnSOD-deficient mice. Mol Cell Biochem 353:151–157.

Cagnone GL, Dufort I, Vigneault C, Sirard MA. 2012. Differential gene expression profile in bovine blastocysts resulting from hyperglycemia exposure during early cleavage stages. Biol Reprod 86:50.

Cai W, Ramdas M, Zhu L, Chen X, Striker GE, Vlassara H. 2012. Oral advanced glycation endproducts (AGEs) promote insulin resistance and diabetes by depleting the antioxidant defenses AGE receptor-1 and sirtuin 1. Proc Natl Acad Sci USA 109: 15888–15893.

Caniggia I, Grisaru-Gravnosky S, Kuliszewsky M, Post M, Lye SJ. 1999. Inhibition of TGF-beta 3 restores the invasive capability of extravillous trophoblasts in preeclamptic pregnancies. J Clin Invest 103:1641–1650.

Cervera AM, Bayley JP, Devilee P, McCreath KJ. 2009. Inhibition of succinate dehydrogenase dysregulates histone modification in mammalian cells. Mol Cancer 8:89.

Chakrabarty A, Roberts MR. 2007. Ets-2 and C/EBP-beta are important mediators of ovine trophoblast Kunitz domain protein-1 gene expression in trophoblast. BMC Mol Biol 8:14.

Chao CC, Ma YS, Stadtman ER. 1997. Modification of protein surface hydrophobicity and methionine oxidation by oxidative systems. Proc Natl Acad Sci USA 94:2969–2974.

Chi MM, Hoehn A, Moley KH. 2002. Metabolic changes in the glucose-induced apoptotic blastocyst suggest alterations in mitochondrial physiology. Am J Physiol Endocrinol Metab 283:E226–E232.

Cote I, Vigneault C, Laflamme I, Laquerre J, Fournier E, Gilbert I, Scantland S, Gagne D, Blondin P, Robert C. 2011. Comprehensive cross production system assessment of the impact of in vitro microenvironment on the expression of messengers and long non-coding RNAs in the bovine blastocyst. Reproduction 142:99–112.

Cui Y, Kim DS, Park SH, Yoon JA, Kim SK, Kwon SB, Park KC. 2004. Involvement of ERK AND p38 MAP kinase in AAPH-induced COX-2 expression in HaCaT cells. Chem Phys Lipids 129:43–52.

Cui ZJ, Han ZQ, Li ZY. 2011. Modulating protein activity and cellular function by methionine residue oxidation. Amino Acids 43: 505–517.

de Matos DG, Furnus CC, Moses DF, Martinez AG, Matkovic M. 1996. Stimulation of glutathione synthesis of in vitro matured bovine oocytes and its effect on embryo development and freezability. Mol Reprod Dev 45:451–457.

De Palma S, Ripamonti M, Vigano A, Moriggi M, Capitanio D, Samaja M, Milano G, Cerretelli P, Wait R, Gelfi C. 2007. Metabolic modulation induced by chronic hypoxia in rats using a comparative proteomic analysis of skeletal muscle tissue. J Proteome Res 6:1974–1984.

Deban L, Jaillon S, Garlanda C, Bottazzi B, Mantovani A. 2011. Pentraxins in innate immunity: Lessons from PTX3. Cell Tissue Res 343:237–249.

Delekta PC, Apel IJ, Gu S, Siu K, Hattori Y, McAllister-Lucas LM, Lucas PC. 2010. Thrombin-dependent NF-{kappa}B activation and monocyte/endothelial adhesion are mediated by the CARMA3. Bcl10.MALT1 signalosome. J Biol Chem 285: 41432–41442.

Dimova EY, Samoylenko A, Kietzmann T. 2004. Oxidative stress and hypoxia: Implications for plasminogen activator inhibitor-1 expression. Antioxid Redox Signal 6:777–791.

Donnay I, Leese HJ. 1999. Embryo metabolism during the expansion of the bovine blastocyst. Mol Reprod Dev 53:171–178.

Duranthon V, Watson AJ, Lonergan P. 2008. Preimplantation embryo programming: Transcription, epigenetics, and culture environment. Reproduction 135:141–150.

Edwards IJ. 2012. Proteoglycans in prostate cancer. Nat Rev Urol 9:196–206.

Edwards AK, van den Heuvel MJ, Wessels JM, Lamarre J, Croy BA, Tayade C. 2011. Expression of angiogenic basic fibroblast growth factor, platelet derived growth factor, thrombospondin-1 and their receptors at the porcine maternal-fetal interface. Reprod Biol Endocrinol 9:5.

El-Sayed A, Hoelker M, Rings F, Salilew D, Jennen D, Tholen E, Sirard MA, Schellander K, Tesfaye D. 2006. Large-scale transcriptional analysis of bovine embryo biopsies in relation to pregnancy success after transfer to recipients. Physiol Genomics 28:84–96.

El-Tanani MK, Jin D, Campbell FC, Johnston PG. 2010. Interferon-induced transmembrane 3 binds osteopontin in vitro: Expressed in vivo IFITM3 reduced OPN expression. Oncogene 29: 752–762.

Farin PW, Piedrahita JA, Farin CE. 2006. Errors in development of fetuses and placentas from in vitro-produced bovine embryos. Theriogenology 65:178–191.

Feugang JM, Van Langendonckt A, Sayoud H, Rees JF, Pampfer S, Moens A, Dessy F, Donnay I. 2003. Effect of prooxidant agents added at the morula/blastocyst stage on bovine embryo development, cell death and glutathione content. Zygote 11: 107–118.

Feugang JM, Donnay I, Mermillod P, Marchandise J, Lequarre AS. 2005. Impact of pro-oxidant agents on the morula-blastocyst transition in bovine embryos. Mol Reprod Dev 71: 339–346.

Fischer B, Bavister BD. 1993. Oxygen tension in the oviduct and uterus of rhesus monkeys, hamsters and rabbits. J Reprod Fertil 99:673–679.

Gardiner CS, Reed DJ. 1994. Status of glutathione during oxidant-induced oxidative stress in the preimplantation mouse embryo. Biol Reprod 51:1307–1314.

Gardiner CS, Reed DJ. 1995a. Glutathione redox cycle-driven recovery of reduced glutathione after oxidation by tertiary-butyl hydroperoxide in preimplantation mouse embryos. Arch Biochem Biophys 321:6–12.

Gardiner CS, Reed DJ. 1995b. Synthesis of glutathione in the preimplantation mouse embryo. Arch Biochem Biophys 318: 30–36.

Gardiner CS, Salmen JJ, Brandt CJ, Stover SK. 1998. Glutathione is present in reproductive tract secretions and improves development of mouse embryos after chemically induced glutathione depletion. Biol Reprod 59:431–436.

Guerin P, El Mouatassim S, Menezo Y. 2001. Oxidative stress and protection against reactive oxygen species in the pre-implantation embryo and its surroundings. Hum Reprod Update 7:175–189.

Hamaguchi T, Iizuka N, Tsunedomi R, Hamamoto Y, Miyamoto T, Iida M, Tokuhisa Y, Sakamoto K, Takashima M, Tamesa T, Oka M. 2008. Glycolysis module activated by hypoxia-inducible factor 1alpha is related to the aggressive phenotype of hepatocellular carcinoma. Int J Oncol 33:725–731.

Hamatani T, Ko M, Yamada M, Kuji N, Mizusawa Y, Shoji M, Hada T, Asada H, Maruyama T, Yoshimura Y. 2006. Global gene expression profiling of preimplantation embryos. Hum Cell 19:98–117.

Hannan NJ, Salamonsen LA. 2008. CX3CL1 and CCL14 regulate extracellular matrix and adhesion molecules in the trophoblast: Potential roles in human embryo implantation. Biol Reprod 79:58–65.

Harvey AJ, Kind KL, Thompson JG. 2002. REDOX regulation of early embryo development. Reproduction 123:479–486.

Hashimoto S, Minami N, Yamada M, Imai H. 2000. Excessive concentration of glucose during in vitro maturation impairs the developmental competence of bovine oocytes after in vitro fertilization: Relevance to intracellular reactive oxygen species and glutathione contents. Mol Reprod Dev 56:520–526.

Hayashi Y, Call MK, Chikama T, Liu H, Carlson EC, Sun Y, Pearlman E, Funderburgh JL, Babcock G, Liu CY, Ohashi Y, Kao WW. 2010. Lumican is required for neutrophil extravasation following corneal injury and wound healing. J Cell Sci 123:2987–2995.

Huang da W, Sherman BT, Lempicki RA. 2009a. Bioinformatics enrichment tools: Paths toward the comprehensive functional analysis of large gene lists. Nucleic Acids Res 37:1–13.

Huang da W, Sherman BT, Lempicki RA. 2009b. Systematic and integrative analysis of large gene lists using DAVID bioinformatics resources. Nat Protoc 4:44–57.

Jaleel MA, Tsai AC, Sarkar S, Freedman PV, Rubin LP. 2004. Stromal cell-derived factor-1 (SDF-1) signalling regulates human placental trophoblast cell survival. Mol Hum Reprod 10:901–909.

Jinnin M, Ihn H, Mimura Y, Asano Y, Yamane K, Tamaki K. 2005. Regulation of fibrogenic/fibrolytic genes by platelet-derived growth factor C, a novel growth factor, in human dermal fibroblasts. J Cell Physiol 202:510–517.

Johnson GA, Burghardt RC, Bazer FW, Spencer TE. 2003. Osteopontin: Roles in implantation and placentation. Biol Reprod 69:1458–1471.

Karja NW, Kikuchi K, Fahrudin M, Ozawa M, Somfai T, Ohnuma K, Noguchi J, Kaneko H, Nagai T. 2006. Development to the blastocyst stage, the oxidative state, and the quality of early developmental stage of porcine embryos cultured in alteration of glucose concentrations in vitro under different oxygen tensions. Reprod Biol Endocrinol 4:54.

Kawamura K, Kawamura N, Kumagai J, Fukuda J, Tanaka T. 2007. Tumor necrosis factor regulation of apoptosis in mouse preimplantation embryos and its antagonism by transforming growth factor alpha/phosphatidylionsitol 3-kinase signaling system. Biol Reprod 76:611–618.

Kim JY, Song EH, Lee HJ, Oh YK, Choi KH, Yu DY, Park SI, Seong JK, Kim WH. 2010. HBx-induced hepatic steatosis and apoptosis are regulated by TNFR1- and NF-kappaB-dependent pathways. J Mol Biol 397:917–931.

Kopp A, Bala M, Buechler C, Falk W, Gross P, Neumeier M, Scholmerich J, Schaffler A. 2010. C1q/TNF-related protein-3 represents a novel and endogenous lipopolysaccharide antagonist of the adipose tissue. Endocrinology 151:5267–5278.

Krisher RL, Prather RS. 2012. A role for the Warburg effect in preimplantation embryo development: Metabolic modification to support rapid cell proliferation. Mol Reprod Dev 79:311–320.

Kubo H, Spindle A, Pedersen RA. 1981. Inhibition of mouse blastocyst attachment and outgrowth by protease inhibitors. J Exp Zool 216:445–451.

Kurzawa R, Glabowski W, Baczkowski T, Wiszniewska B, Marchlewicz M. 2004. Growth factors protect in vitro cultured embryos from the consequences of oxidative stress. Zygote 12:231–240.

Kwong WY, Adamiak SJ, Gwynn A, Singh R, Sinclair KD. 2010. Endogenous folates and single-carbon metabolism in the ovarian follicle, oocyte and pre-implantation embryo. Reproduction 139:705–715.

Lazzari G, Wrenzycki C, Herrmann D, Duchi R, Kruip T, Niemann H, Galli C. 2002. Cellular and molecular deviations in bovine in vitro-produced embryos are related to the large offspring syndrome. Biol Reprod 67:767–775.

Lee HR, Cho JM, Shin DH, Yong CS, Choi HG, Wakabayashi N, Kwak MK. 2008. Adaptive response to GSH depletion and resistance to L-buthionine-(S,R)-sulfoximine: Involvement of Nrf2 activation. Mol Cell Biochem 318:23–31.

Leese HJ, Sturmey RG, Baumann CG, McEvoy TG. 2007. Embryo viability and metabolism: Obeying the quiet rules. Hum Reprod 22:3047–3050.

Leipnitz G, Solano AF, Seminotti B, Amaral AU, Fernandes CG, Beskow AP, Dutra Filho CS, Wajner M. 2009. Glycine provokes lipid oxidative damage and reduces the antioxidant defenses in brain cortex of young rats. Cell Mol Neurobiol 29:253–261.

Lequarre AS, Marchandise J, Moreau B, Massip A, Donnay I. 2003. Cell cycle duration at the time of maternal zygotic transition for in vitro produced bovine embryos: Effect of oxygen tension and transcription inhibition. Biol Reprod 69:1707–1713.

Leunda-Casi A, Genicot G, Donnay I, Pampfer S, De Hertogh R. 2002. Increased cell death in mouse blastocysts exposed to high D-glucose in vitro: Implications of an oxidative stress and alterations in glucose metabolism. Diabetologia 45:571–579.

Li G, Khateeb K, Schaeffer E, Zhang B, Khatib H. 2012. Genes of the transforming growth factor-beta signalling pathway are associated with pre-implantation embryonic development in cattle. J Dairy Res 79:310–317.

Liu RM. 2008. Oxidative stress, plasminogen activator inhibitor 1, and lung fibrosis. Antioxid Redox Signal 10:303–319.

Liu L, Trimarchi JR, Keefe DL. 1999. Thiol oxidation-induced embryonic cell death in mice is prevented by the antioxidant dithiothreitol. Biol Reprod 61:1162–1169.

Lohr K, Sardana H, Lee S, Wu F, Huso DL, Hamad AR, Chakravarti S. 2012. Extracellular matrix protein lumican regulates inflammation in a mouse model of colitis. Inflamm Bowel Dis 18:143–151.

Lott WM, Anchamparuthy VM, McGilliard ML, Mullarky IK, Gwazdauskas FC. 2011. Influence of cysteine in conjunction with growth factors on the development of in vitro-produced bovine embryos. Reprod Domest Anim 46:585–594.

Loureiro B, Brad AM, Hansen PJ. 2007. Heat shock and tumor necrosis factor-alpha induce apoptosis in bovine preimplantation embryos through a caspase-9-dependent mechanism. Reproduction 133:1129–1137.

Luhmann UF, Meunier D, Shi W, Luttges A, Pfarrer C, Fundele R, Berger W. 2005. Fetal loss in homozygous mutant Norrie disease mice: A new role of Norrin in reproduction. Genesis 42: 253–262.

Luna C, Li G, Qiu J, Epstein DL, Gonzalez P. 2009. Role of miR-29b on the regulation of the extracellular matrix in human trabecular meshwork cells under chronic oxidative stress. Mol Vis 15: 2488–2497.

Marin-Hernandez A, Gallardo-Perez JC, Ralph SJ, Rodriguez-Enriquez S, Moreno-Sanchez R. 2009. HIF-1alpha modulates energy metabolism in cancer cells by inducing over-expression of specific glycolytic isoforms. Mini Rev Med Chem 9:1084–1101.

Marotta M, Ruiz-Roig C, Sarria Y, Peiro JL, Nunez F, Ceron J, Munell F, Roig-Quilis M. 2009. Muscle genome-wide expression profiling during disease evolution in mdx mice. Physiol Genomics 37:119–132.

Martin-Romero FJ, Miguel-Lasobras EM, Dominguez-Arroyo JA, Gonzalez-Carrera E, Alvarez IS. 2008. Contribution of culture media to oxidative stress and its effect on human oocytes. Reprod Biomed Online 17:652–661.

Massague J, Chen YG. 2000. Controlling TGF-beta signaling. Genes Dev 14:627–644.

Meade ES, Ma YY, Guller S. 2007. Role of hypoxia-inducible transcription factors 1alpha and 2alpha in the regulation of plasminogen activator inhibitor-1 expression in a human trophoblast cell line. Placenta 28:1012–1019.

Menkhorst EM, Lane N, Winship AL, Li P, Yap J, Meehan K, Rainczuk A, Stephens A, Dimitriadis E. 2012. Decidual-secreted factors alter invasive trophoblast membrane and secreted proteins implying a role for decidual cell regulation of placentation. PLoS ONE 7:e31418.

Mueller C, Baudler S, Welzel H, Bohm M, Nickenig G. 2002. Identification of a novel redox-sensitive gene, Id3, which mediates angiotensin II-induced cell growth. Circulation 105: 2423–2428.

Nguyen VD, Saaranen MJ, Karala AR, Lappi AK, Wang L, Raykhel IB, Alanen HI, Salo KE, Wang CC, Ruddock LW. 2011. Two endoplasmic reticulum PDI peroxidases increase the efficiency

of the use of peroxide during disulfide bond formation. J Mol Biol 406:503–515.

Nickenig G, Baudler S, Muller C, Werner C, Werner N, Welzel H, Strehlow K, Bohm M. 2002. Redox-sensitive vascular smooth muscle cell proliferation is mediated by GKLF and Id3 in vitro and in vivo. FASEB J 16:1077–1086.

Oda M, Kure S, Sugawara T, Yamaguchi S, Kojima K, Shinka T, Sato K, Narisawa A, Aoki Y, Matsubara Y, Omae T, Mizoi K, Kinouchi H. 2007. Direct correlation between ischemic injury and extracellular glycine concentration in mice with genetically altered activities of the glycine cleavage multienzyme system. Stroke 38:2157–2164.

Osterlund C, Wramsby H, Pousette A. 1996. Temporal expression of platelet-derived growth factor (PDGF)-A and its receptor in human preimplantation embryos. Mol Hum Reprod 2:507–512.

Paczkowski M, Krisher R. 2010. Aberrant protein expression is associated with decreased developmental potential in porcine cumulus-oocyte complexes. Mol Reprod Dev 77:51–58.

Pantaleon M, Tan HY, Kafer GR, Kaye PL. 2010. Toxic effects of hyperglycemia are mediated by the hexosamine signaling pathway and o-linked glycosylation in early mouse embryos. Biol Reprod 82:751–758.

Plourde D, Vigneault C, Lemay A, Breton L, Gagne D, Laflamme I, Blondin P, Robert C. 2012. Contribution of oocyte source and culture conditions to phenotypic and transcriptomic variation in commercially produced bovine blastocysts. Theriogenology 78:116–131; e111–e113.

Rehman AO, Wang CY. 2009. CXCL12/SDF-1 alpha activates NF-kappaB and promotes oral cancer invasion through the Carma3/Bcl10/Malt1 complex. Int J Oral Sci 1:105–118.

Rizos D, Lonergan P, Boland MP, Arroyo-Garcia R, Pintado B, de la Fuente J, Gutierrez-Adan A. 2002. Analysis of differential messenger RNA expression between bovine blastocysts produced in different culture systems: Implications for blastocyst quality. Biol Reprod 66:589–595.

Robert C, Nieminen J, Dufort I, Gagne D, Grant JR, Cagnone G, Plourde D, Nivet AL, Fournier E, Paquet E, Blazejczyk M, Rigault P, Juge N, Sirard MA. 2011. Combining resources to obtain a comprehensive survey of the bovine embryo transcriptome through deep sequencing and microarrays. Mol Reprod Dev 78:651–664.

Rodina TM, Cooke FN, Hansen PJ, Ealy AD. 2009. Oxygen tension and medium type actions on blastocyst development and interferon-tau secretion in cattle. Anim Reprod Sci 111:173–188.

Rodriguez-Zas SL, Schellander K, Lewin HA. 2008. Biological interpretations of transcriptomic profiles in mammalian oocytes and embryos. Reproduction 135:129–139.

Sakatani M, Yamanaka K, Kobayashi S, Takahashi M. 2008. Heat shock-derived reactive oxygen species induce embryonic mortality in in vitro early stage bovine embryos. J Reprod Dev 54:496–501.

Santra M, Santra S, Zhang J, Chopp M. 2008. Ectopic decorin expression up-regulates VEGF expression in mouse cerebral endothelial cells via activation of the transcription factors Sp1, HIF1alpha, and Stat3. J Neurochem 105:324–337.

Schaefer L, Raslik I, Grone HJ, Schonherr E, Macakova K, Ugorcakova J, Budny S, Schaefer RM, Kresse H. 2001. Small proteoglycans in human diabetic nephropathy: Discrepancy between glomerular expression and protein accumulation of decorin, biglycan, lumican, and fibromodulin. FASEB J 15: 559–561.

Siegrist F, Ebeling M, Certa U. 2011. The small interferon-induced transmembrane genes and proteins. J Interferon Cytokine Res 31:183–197.

Singh M, Moniri NH. 2012. Reactive oxygen species are required for beta2 adrenergic receptor-beta-arrestin interactions and signaling to ERK1/2. Biochem Pharmacol 84:661–669.

Smith S, Francis R, Guilbert L, Baker PN. 2002. Growth factor rescue of cytokine mediated trophoblast apoptosis. Placenta 23:322–330.

Smith C, Berg D, Beaumont S, Standley NT, Wells DN, Pfeffer PL. 2007. Simultaneous gene quantitation of multiple genes in individual bovine nuclear transfer blastocysts. Reproduction 133:231–242.

Smith SL, Everts RE, Sung LY, Du F, Page RL, Henderson B, Rodriguez-Zas SL, Nedambale TL, Renard JP, Lewin HA, Yang X, Tian XC. 2009. Gene expression profiling of single bovine embryos uncovers significant effects of in vitro maturation, fertilization and culture. Mol Reprod Dev 76:38–47.

Steele W, Allegrucci C, Singh R, Lucas E, Priddle H, Denning C, Sinclair K, Young L. 2005. Human embryonic stem cell methyl cycle enzyme expression: Modelling epigenetic programming in assisted reproduction? Reprod Biomed Online 10:755–766.

Stover SK, Gushansky GA, Salmen JJ, Gardiner CS. 2000. Regulation of gamma-glutamate-cysteine ligase expression by oxidative stress in the mouse preimplantation embryo. Toxicol Appl Pharmacol 168:153–159.

Sugiura K, Pendola FL, Eppig JJ. 2005. Oocyte control of metabolic cooperativity between oocytes and companion granulosa cells: Energy metabolism. Dev Biol 279:20–30.

Suo G, Jiang Y, Cowan B, Wang JY. 2009. Platelet-derived growth factor C is upregulated in human uterine fibroids and regulates uterine smooth muscle cell growth. Biol Reprod 81:749–758.

Takahashi M, Nagai T, Hamano S, Kuwayama M, Okamura N, Okano A. 1993. Effect of thiol compounds on in vitro development and intracellular glutathione content of bovine embryos. Biol Reprod 49:228–232.

Thieme R, Schindler M, Ramin N, Fischer S, Muhleck B, Fischer B, Navarrete Santos A. 2012. Insulin growth factor adjustment in preimplantation rabbit blastocysts and uterine tissues in response to maternal type 1 diabetes. Mol Cell Endocrinol 358:96–103.

Thompson JG. 2000. In vitro culture and embryo metabolism of cattle and sheep embryos---A decade of achievement. Anim Reprod Sci 6:263–275.

Urtasun R, Lopategi A, George J, Leung TM, Lu Y, Wang X, Ge X, Fiel MI, Nieto N. 2012. Osteopontin, an oxidant stress sensitive cytokine, up-regulates collagen-I via integrin alpha(V)beta(3) engagement and PI3K/pAkt/NFkappaB signaling. Hepatology 55:594–608.

Vandesompele J, De Preter K, Pattyn F, Poppe B, Van Roy N, De Paepe A, Speleman F. 2002. Accurate normalization of real-time quantitative RT-PCR data by geometric averaging of multiple internal control genes. Genome Biol 3:RESEARCH0034.

Verrecchia F, Mauviel A. 2002. Transforming growth factor-beta signaling through the Smad pathway: Role in extracellular matrix gene expression and regulation. J Invest Dermatol 118:211–215.

Vigneault C, McGraw S, Massicotte L, Sirard MA. 2004. Transcription factor expression patterns in bovine in vitro-derived embryos prior to maternal-zygotic transition. Biol Reprod 70:1701–1709.

Weissbach H, Etienne F, Hoshi T, Heinemann SH, Lowther WT, Matthews B, St John G, Nathan C, Brot N. 2002. Peptide methionine sulfoxide reductase: Structure, mechanism of action, and biological function. Arch Biochem Biophys 397:172–178.

Wikstrom AK, Nash P, Eriksson UJ, Olovsson MH. 2009. Evidence of increased oxidative stress and a change in the plasminogen activator inhibitor (PAI)-1 to PAI-2 ratio in early-onset but not late-onset preeclampsia. Am J Obstet Gynecol 201:597;e591–e598.

Yang L, Serada S, Fujimoto M, Terao M, Kotobuki Y, Kitaba S, Matsui S, Kudo A, Naka T, Murota H, Katayama I. 2012. Periostin facilitates skin sclerosis via PI3K/Akt dependent mechanism in a mouse model of scleroderma. PLoS ONE 7:e41994.

Yoshida Y, Itoh N, Saito Y, Hayakawa M, Niki E. 2004. Application of water-soluble radical initiator, 2,2′-azobis[2-(2-imidazolin-2-yl) propane] dihydrochloride, to a study of oxidative stress. Free Radic Res 38:375–384.

Young LE, Sinclair KD, Wilmut I. 1998. Large offspring syndrome in cattle and sheep. Rev Reprod 3:155–163.

Zhang C, Liu C, Li D, Yao N, Yuan X, Yu A, Lu C, Ma X. 2009. Intracellular redox imbalance and extracellular amino acid metabolic abnormality contribute to arsenic-induced developmental retardation in mouse preimplantation embryos. J Cell Physiol 222:444–455.

Zhang C, Jia P, Jia Y, Li Y, Webster KA, Huang X, Achary M, Lemanski SL, Lemanski LF. 2011. Anoxia, acidosis, and intergenic interactions selectively regulate methionine sulfoxide reductase transcriptions in mouse embryonic stem cells. J Cell Biochem 112:98–106.

Zhao M, Wimmer A, Trieu K, Discipio RG, Schraufstatter IU. 2004. Arrestin regulates MAPK activation and prevents NADPH oxidase-dependent death of cells expressing CXCR2. J Biol Chem 279:49259–49267.

Zheng Z, Jia JL, Bou G, Hu LL, Wang ZD, Shen XH, Shan ZY, Shen JL, Liu ZH, Lei L. 2012. rRNA genes are not fully activated in mouse somatic cell nuclear transfer embryos. J Biol Chem 287:19949–19960.